COPYRIGHT NOTICE

This is the peer-reviewed version of the following article:

Yengejeh, H., Shahnia, F., Islam, S. (2015) Disconnection time and sequence of rooftop PVs under short-circuit faults in low voltage networks, North American Power Symposium, NAPS 2015; Charlotte, United States; 4th-6th October 2015 p. 1-6.

Which has been published in final form at:
https://doi.org/10.1109/NAPS.2015.7335127

Disconnection Time and Sequence of Rooftop PVs under Short-circuit Faults in Low Voltage Networks

Hadi Hosseinian Yengejeh, *Student Member, IEEE*, Farhad Shahnia, *Senior Member, IEEE*, Syed M. Islam, *Senior Member, IEEE*

Department of Electrical and Computer Engineering, Curtin University, Perth, Australia

hadi.hosseinian@curtin.edu.au, farhad.shahnia@curtin.edu.au, s.islam@curtin.edu.au

***Abstract*—This paper presents an analysis on the disconnection time of single-phase rooftop PVs, located in a three-phase four-wire low voltage distribution feeder after a line-to-ground short-circuit fault on the low voltage feeder. The paper aims to evaluate and discuss the disconnection time and sequence of PVs in a network with 100% PV penetration level. The impact of different parameters such as the location of the fault, impedance of the fault and the ratio of PVs generation capacity to the load demand are considered. Furthermore, the effect of the system earthing in the form of multiple earthed neutral and non-effectively grounded systems are evaluated on the PVs disconnection time. The analyses intend to figure out the conditions under which the PVs in the feeder may fail to disconnect after a line-to-ground fault and keep feeding the fault. The analyses are carried out in PSCAD/EMTDC software.**

***Index Terms*—Rooftop PVs, Short-circuit faults, Voltage profile, Multiple earthed neutral.**

I. INTRODUCTION

During the last decade, a vast effort has been made towards the expansion and increase in the penetration level of distributed generation (DG) units within the electric distribution networks. Single-phase rooftop photovoltaics cells (PVs) are the most commonly utilized type of DGs that are installed in distribution networks of many countries. As an example, in the last 6 years, over one million rooftop PVs have been installed in Australia [1]. However, the increasing penetration level of these units in low voltage distribution networks has imposed several technical problems such voltage rise issues [2, 3] and power quality problems [4, 5]. The technical and economic impacts of imposed over-voltages by rooftop PVs in PV dominated distribution feeders is considered in [2-5] and several improvement techniques are proposed in [6] to mitigate or minimize these problems. Furthermore, the sudden variations of voltage in the PV dominated feeders as the result of clouding has been studied in [7] where some improvement methods are proposed in [8] to overcome rapid voltage fluctuations.

In addition to voltage rise, fluctuation and power quality problems, the utilities worldwide are concerned with the impact of high penetration of rooftop PVs on the mis-coordination among the protective devices in those networks [9-12]. As an example, reference [13] has discussed the protection problems related to the high penetration of rooftop PVs in distribution networks. For medium voltage (MV) networks with high penetration of rooftop PVs in their low voltage (LV) feeders, reference [14] proposes a new technique to define and update the settings of the network protective devices to maintain a proper coordination among them. In addition, reference [15] proposes a new technique based on current phase comparison at different points along the MV feeders to detect the contribution of rooftop PVs on the short circuit faults.

The above references have focused on the impact of the rooftop PVs on MV feeders but have not discussed the PVs effects on the LV feeders to which they are connected. In addition, they have not considered the unequal distribution of PV among the phases neither the different nominal ratings of the PVs in a feeder. These points need to be considered in protection-related studies of networks with high penetration of PVs.

On the other hand, the utilities try to minimize the possible impacts of rooftop PVs by limiting their penetration in the networks. As an example, majority of electrical utilities in Australia, have developed a 30% maximum penetration limit for the single-phase rooftop PVs in each LV feeder [16]. This limit prevents newer householders to install rooftop PVs. From protection side, the utilities are worried that due to high penetration of rooftop PVs, there is a possibility that the rooftop PVs do not allow the voltage along the feeder to drop during short-circuit faults, resulting in the continuous supply of the fault through the rooftop PVs, even if the upstream circuit breakers have disconnected the upstream.

To facilitate higher penetration of single-phase rooftop PVs in electric networks, the protection issues of these networks should be evaluated in more details. In this regard, this paper focuses on the LV feeder to which the single-phase rooftop PVs are connected and the unequal (number and rating) of PVs in each phase of the three-phase system are considered. In addition, the voltage profile along the feeder after a short-circuit fault in the LV feeder is analyzed carefully. Within this period, the disconnection time and sequence of disconnection of the rooftop PVs are also analyzed. Several parameters such as the impedance of fault (IoF), location of fault (LoF) and PV generation capacity to residential load demand ratio (GDR) are considered within the studies. The voltages of nodes along the feeder are observed during the first few cycles after a fault appearance on the LV networks. Another aim of this paper is to compare the effects of PVs disconnection time with respect to the grounding system of the feeder. The paper will present a comparison on the voltage profile along the feeder in multiple earthed neutral (MEN) [17] and non-effectively grounded (NEG) [18] networks after a short-circuit fault. Only line-to-ground (LG) faults, which are the most common type of faults in distribution networks are considered in the analyses of this

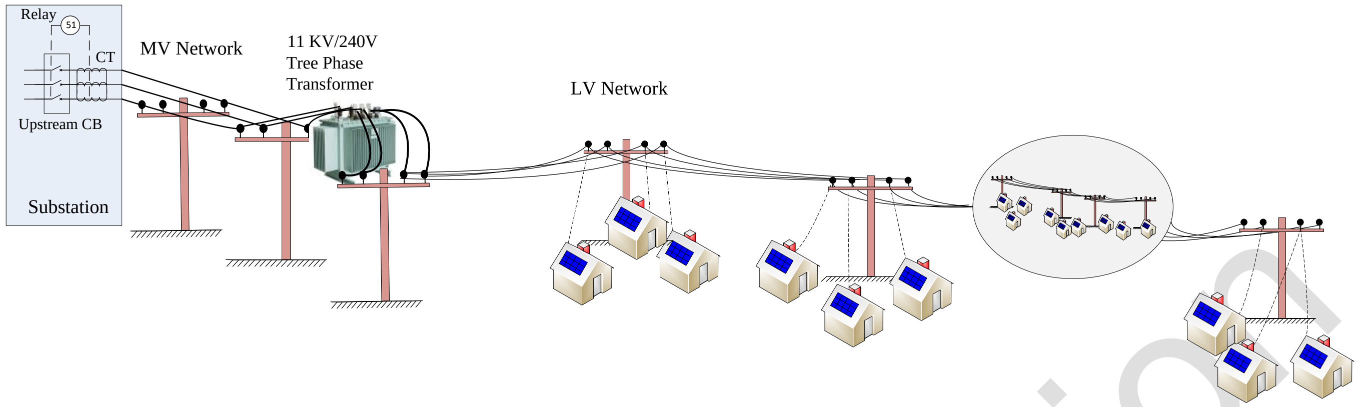

Fig. 1. Schematic diagram of the considered three-phase, four-wire LV feeder with high penetration of rooftop PVs, supplied from an MV feeder.

paper. The main contributions of this research are:

- to evaluate and discuss the disconnection time and sequence of single-phase rooftop PVs distributed in different phases during LG fault,
- to investigate the effect of IoF and LoF on the on the disconnection time of rooftop PVs after an LG fault,
- to investigate the correlation between the disconnection time of PVs and a high GDR under short-circuit scenarios,
- to compare the effect of NEG and MEN systems on the disconnection time of rooftop PVs in a LV network with high penetration of rooftop PVs,
- to define the conditions under which rooftop PVs may not be disconnected after an LG fault in the LV feeder.

The rest of the paper is organized as follows: Section II introduces the LV network under consideration. The research methodology is discussed in Section III and the results of the analyses are presented in Section IV. The general conclusions and findings of the research are highlighted in the last section of the paper.

II. Network Under Consideration

Let us consider the network of Fig. 1 which schematically represents a typical Australian urban LV distribution network, used for supplying residential loads. This system is selected as the case study in this paper. It is assumed that a three-phase three-wire MV feeder supplies a three-phase four-wire LV feeder through a three-phase Dyn distribution transformer [19]. The residential houses are assumed to be single-phase loads connected to the LV feeder. In this research, to consider a worst case scenario, it is assumed that the penetration of single-phase rooftop PVs is 100%. The considered network in this paper is composed of 30 houses, equally distributed among the three phases.

A similar network is used by majority of the European and Asian utilities to supply the urban residential loads. It is to be noted that this system is different from the North American LV residential networks [20].

The new and properly designed LV feeders are in the form of MEN type where the neutral wire is earthed at the secondary of the distribution transformer as well as at each load premises [21], as seen from Fig. 2(a). However, older LV

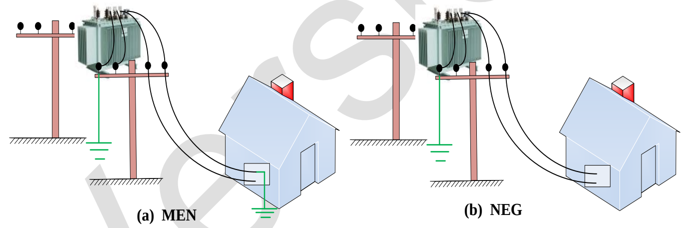

Fig. 2. Schematic diagram of different earthing systems in an LV feeder: (a) MEN system, (b) NEG system

Table 1. The maximum rooftop PV disconnection time in response to abnormal voltages in the feeder.

Voltage (%)	Maximum tripping time (cycle)
50% < V < 88% or 110% < V < 137	120 cycles
V < 50%	6 cycles
V > 137%	2 cycle

feeders or LV feeders developed without proper engineering supervisions may be in the form of an NEG system. To consider this, the network of Fig. 1 is considered assuming the neutral wire is only grounded at the distribution transformer but not at every residential load premises, as seen from Fig. 2(b).

The rooftop PVs are assumed to be as constant single-phase power sources, operating at unity power factor, based on IEEE Recommended Practice for Utility Interface of Photovoltaic (PV) Systems [22]. Furthermore, the current output of the PV are limited to be below 150% of the nominal value during the faults. Each PV is assumed to be 4.4 kW, which is the current median of the most common rooftop PVs sizes in Perth, Western Australia [23].

The loads of the network are assumed to be single-phase and constant impedance type, distributed equally among the phases. Each load is assumed to be 4.4 kVA [24] with a power factor of 0.95, which is equal to the after diversity maximum demand (ADMD) of the town houses and villas in Perth, Western Australia.

It is to be noted that the considered system is composed of 30 houses supplied by a 150 kVA transformer. Three houses are assumed to be supplied from each pole, where the poles are located with a distance of 40 meters from each other.

III. Research Methodology

IEEE Recommended Practice for Utility Interface of Photovoltaic (PV) Systems [22] defines the normal and abnormal operating voltage boundaries for the rooftop PVs of smaller than 10 kW. Based on this standard, the rooftop PVs should be isolated and disconnected from the LV feeder and do not energize it if the feeder voltage drops below 88% of the nominal voltage. The maximum time for the PVs disconnection depends on the level of the voltage drop, as given in Table 1. In a similar fashion, the PVs should also get isolated if the feeder voltage rises above 110% of the nominal voltage.

It is expected that following a short-circuit LG fault in the LV feeder, the voltage along the feeder in the faulty-phase will drop quickly while the voltage in the other (healthy) phases will rise. The level of the voltage drop in the faulty phase mainly depends on the fault impedance. The current concern of utilities is that the high PV generation to load demand ratio, earthing of the system as well as the fault impedance and location may cause the voltage drop not to be below 88% of the nominal voltage. If it happens so, the rooftop PVs will not detect any abnormal voltage in the feeder and will not get disconnected. This will allow the PVs to continue to feed the fault. Under such scenarios, the voltage in the other (healthy) phases may also not rise above the threshold of 110%; hence the PVs on the healthy phase(s) may continue to supply the fault via the distribution transformer. The above-mentioned scenario will continue until the upstream circuit breaker, which is usually controlled by an inverse definite minimum time (IDMT) over current relay, trips the circuit. After the upstream circuit breaker has tripped the circuit, the voltages in both faulty and healthy phases will significantly drop, leading to the disconnection of the PVs that are still connected. It is worth mentioning that there is a possibility that the fault current to be very small, resulting in being non-detectable with normal overcurrent relays. Thus, the fault will be kept feeding by the upstream network and PVs. These scenarios and situations will be investigated in the Sections IV, V and VI of this paper and then discussed and concluded in Sections VII and VIII.

It is to be noted that although recently developed LV feeders are usually in the form of multiple earthed neutral (MEN) type, the old LV feeders may be non-effectively grounded (NEG). Each of these earthing systems, might have a strong impact on the voltage profile along the feeder following a short-circuit LG faults.

To understand the network situation after a short-circuit LG fault, this paper considers the network given in Fig. 1 and evaluates the voltage along the feeder and the disconnection time of the PVs based on the following four parameters:

- PV Generation capacity to load demand ratio (GDR)
- impedance of fault (IoF)
- location of fault (LoF) along the feeder
- network earthing system.

Several simulation case studies are considered and developed in PSCAD/EMTDC to evaluate the system performance. To analyze each parameter, the selected cases are re-examined assuming the other parameters as constant and the results (i.e. the voltage along the feeder following a short-circuit LG fault and the disconnection time and sequence of the PVs) are recorded. At the end, the results are tabulated and evaluated.

IV. Impact of Impedance of Fault (IoF)

Let us consider the network of Fig. 1 with the GDR of unity. A short-circuit LG fault is applied at the middle of phase-a (i.e. LoF = node 5). In this study, the IoF is varied from a very small (0.002 and 0.2 Ω) to small (1 and 2 Ω) and high (20 Ω) values. The voltage profile along the feeder after fault occurrence until the disconnection of PVs or the opening of the upstream circuit breaker is shown in Fig. 3. The results are recorded for the MEN and NEG earthed systems, separately. The left hand graphs of Fig. 3 show the voltages in an NEG system while the right hand side graphs show the voltages in an MEN system.

From this figure, it can be seen that the voltage of the faulty phase (i.e. phase-a in this case) drops below the limit of 88% for all IoFs except IoF = 20 Ω. Hence, all of the PVs in the faulty phase disconnect after the fault occurrence. This is valid for both MEN and NEG systems; however, the voltages of the NEG system remain slightly higher than those for the MEN system. This figure also shows that for high impedances IoFs (e.g. 20 Ω) in the MEN system, the voltage of the healthy phases (phase-b and c in this case) rest within the normal operation bandwidth of 88% to 110%; Thus, the PVs connected to healthy phases will not get disconnected and will continue to feed the fault. This is true for the IoFs larger than 1 Ω in the NEG systems. In case of high impedance short-circuit LG faults (e.g. 20 Ω in this case), the PVs in both healthy and faulty phases will remain connected to the LV feeder and will keep feeding the fault until the upstream circuit breaker trips the circuit.

It is worth mentioning that the voltages shown in Fig. 3 are recorded at one specific moment (i.e. after fault occurrence and before disconnection of PVs or upstream circuit breaker). Thus, this figure does not illustrate the voltages after the disconnection of one or more PVs. Thereby, even if the voltages of some nodes is within the nominal bandwidth of 88% to 110% in Fig. 3, their voltages may exit this bandwidth after the disconnection of one or more PVs. Hence, the disconnection time and sequence of the PVs should also be studied.

Now, let us analyses the disconnection time of the PVs in this system and their sequence. The disconnection time of the PVs depends on the time that their point of common coupling (PCC) voltage drops below 88% or rises above 110% of the nominal voltage. Assuming that the fault occurs at t = 0.3 s, the voltages of the faulty phase drop below 88% of the nominal value immediately; hence, all of the PVs within phase-a disconnect simultaneously at t = 0.3048 s (in less than a cycle). Immediately after the fault occurrence, the voltages of the healthy phases increase. As an example, in the considered study, the voltage of node 1 in phase-b and nodes 1-4 in phase-c increase above 110% of their nominal value at t = 0.3060 and 0.3075 s; thereby the PVs connected to these nodes disconnect at these times. The rest of the PVs connected to phase-b and c disconnect in the same fashion before 0.3137 (in less than a cycle after fault occurrence). The upstream CB, which has an extremely inverse characteristic and a time multiplier setting (TMS) of 0.02 opens at t = 1.606 s (i.e. ≈ 1.3 s after the fault occurrence). The schematic disconnection time of the PVs in the considered study case are shown in Fig. 4.

To consider the disconnection time of PVs and their sequence of disconnection in presence of different IoFs, the recorded results are represented in the Radar diagrams of Fig. 5. The top row of this figure is for the considered NEG system while the bottom row represents the MEN system. It can be seen from these figures that the PVs connected to both healthy and faulty phases do not sense the fault and do not disconnect when the IoF is higher than 2 Ω for the MEN system. This is valid for IoFs larger than 1 Ω in the NEG system. The radar diagrams of Fig. 5 also show that the PVs in each phase operate at approximately the same time (i.e. half a cycle difference) for each IoF. The disconnection time increases as the IoF becomes larger.

V. Impact of Location of Fault (LoF)

To analyze the effect of the LoF on the voltage profile along the feeder and hence the disconnection time and sequence of the rooftop PVs, the previous study is repeated (i.e a short-circuit fault is applied on phase-a where the GDR is unity) assuming that the IoF is very small (i.e. 0.002 Ω) while the LoF is varied from the beginning of feeder towards its end. In the rest of this section, LoF = 1, 5 and 10 respectively represents the fault at the beginning node (i.e. node-1), middle (i.e. node-5) and the end (i.e. node-10).

The voltage profile along the feeder is shown in Fig. 6. This figure shows that for all cases of LoF = 1, 5 and 10, the voltage of the nodes in the faulty phase (i.e. phase-a in this case) are very close to each other and all lower than 20% of the nominal value in the MEN and less than the 40% in the NEG system. Hence, it is expected that the PVs within the faulty phase will disconnect regardless of the fault location along the feeder. Following the fault occurrence, the voltages of the nodes in the healthy phases rise above the threshold of 110% and thus their PVs will disconnect.

An interesting issue can be observed in the results of the NEG system. As it can be seen from Fig. 6, the voltage of some of the nodes in phase-b in the NEG system do not rise above the 110% threshold even for a very small IoF of 0.002 Ω. Thus, the PVs connected to the middle and end nodes of this phase will not disconnected under such conditions. The situation will be even worse when the IoF is larger.

Fig. 7 presents the disconnection time of the PVs in radar diagrams. This figure shows that all of the PVs in both healthy and faulty phase disconnect almost at the same time (i.e. few millisecond differences) and this time is not affected strongly with the LoF. This is valid for both of the MEN and NEG systems.

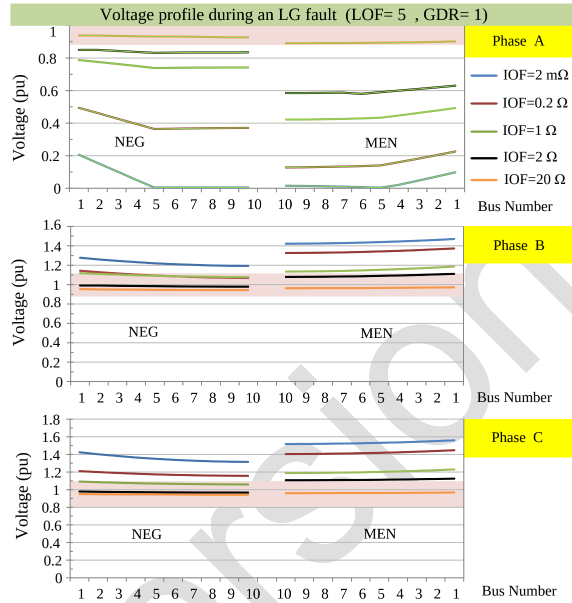

Fig. 3. Voltage profile along the feeder between fault occurrence and the PV/upstream circuit breaker tripping for different IOFs.

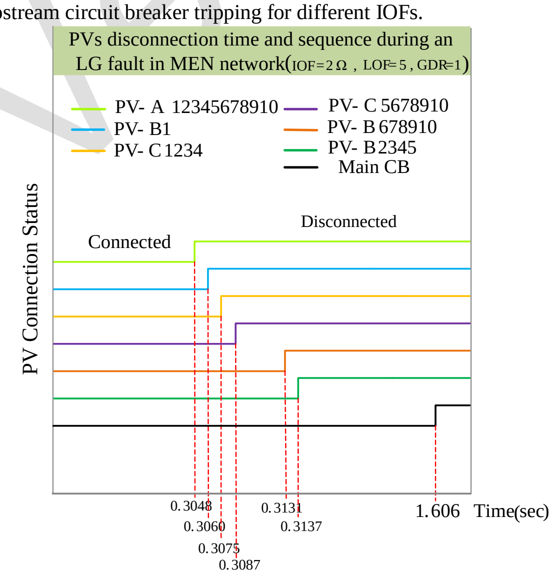

Fig. 4. Disconnection time and sequence of PVs and upstream circuit breaker (CB).

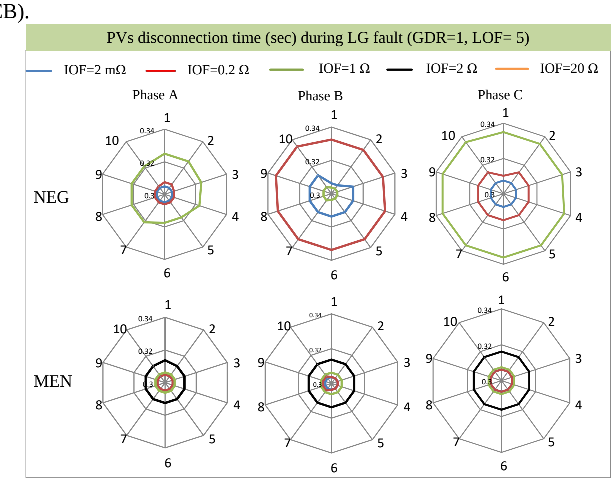

Fig. 5. Disconnection time and sequence of PVs after an LG fault for different IoFs.

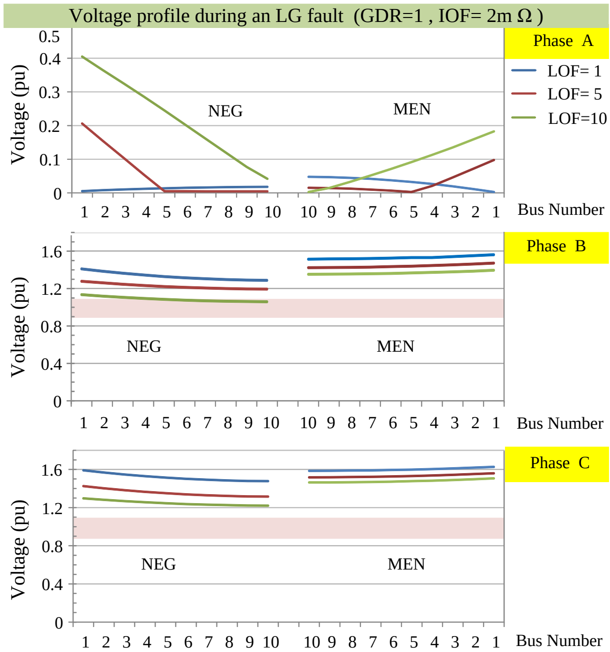

Fig. 6. Voltage profile along the feeder between fault occurrence and the PV/upstream circuit breaker tripping for different LOFs.

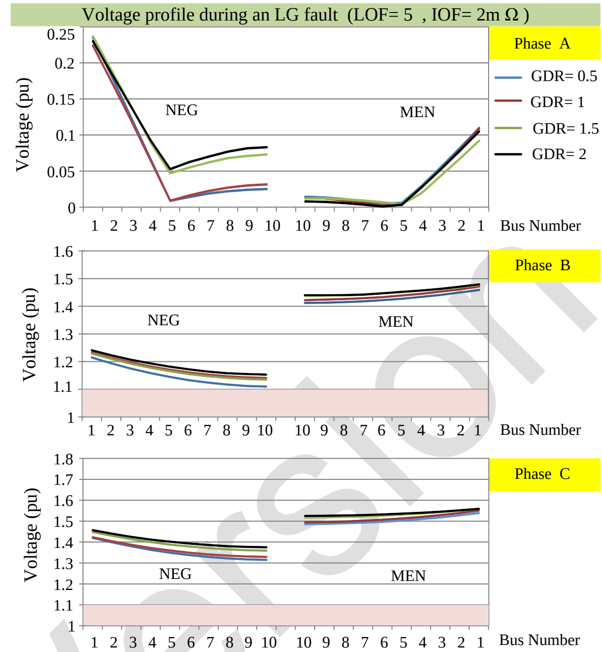

Fig. 8. Voltage profile along the feeder between fault occurrence and the PV/upstream circuit breaker tripping for different GDRs.

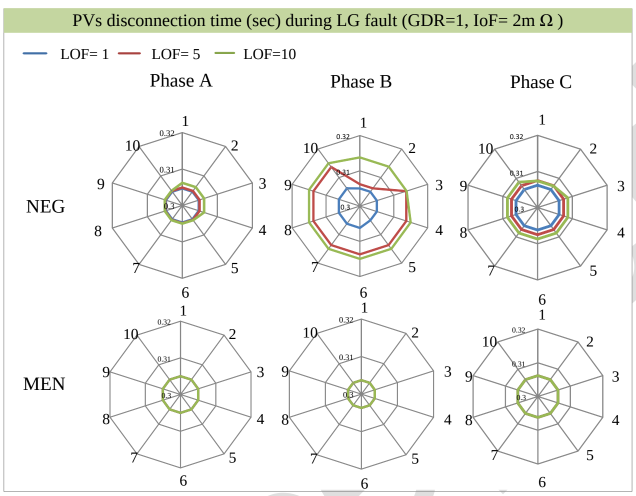

Fig. 7. Disconnection time and sequence of PVs after an LG fault for different LoFs.

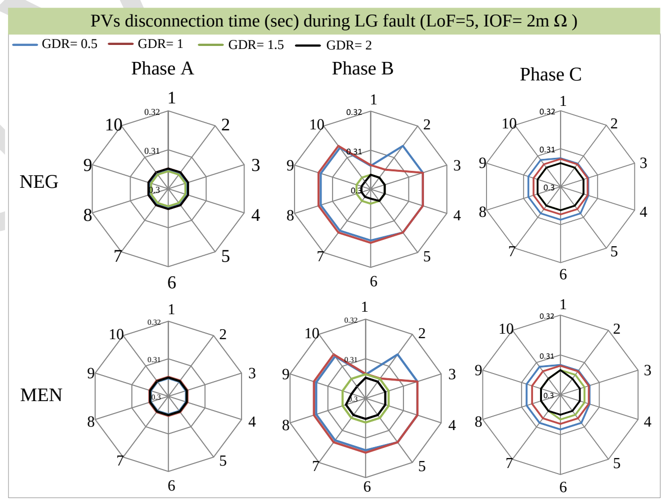

Fig. 9. Time and Sequence of PVs disconnection during an LG in different grounding systems and generation to demand ratios.

VI. Impact of Generation to Demand Ratio (GDR)

To analyze the effect of the GDR on the voltage profile along the feeder and hence the disconnection time and sequence of the rooftop PVs, the previous study is repeated (i.e a short-circuit fault is applied on phase-a with an IoF of 0.002 Ω at the LoF = 5) where the GDR is varied from 50% to 200% in steps of 50%.

The voltage profile along the feeder is shown in Fig. 8. This figure shows that for all different considered GDRs, the voltage of the nodes in the faulty phase (i.e. phase-a in this case) are very close to each other and all lower than 10% of the nominal value in the MEN and less than the 25% in the NEG system. Hence, it is expected that the PVs within the faulty phase will disconnect regardless of the GDR level. Following the fault occurrence, the voltages of the nodes in the healthy phases rise above the threshold of 110%. These voltages are also very close to each other and the PVs connected to these nodes will disconnect.

Fig. 9 presents the disconnection time of the PVs in radar diagrams. It is seen from this figure that as the GDR level increases, the disconnection time of the PVs connected to the healthy phases reduces. This is valid for both of the MEN and NEG systems. The disconnection time of the PVs connected to the faulty phase does not present a specific routine as the GDR level varies; however, all of the PVs disconnect in less than a cycle.

VII. Conclusion and Discussion

An analysis has been carried out to investigate the disconnection time of single-phase rooftop PVs, located in a three-phase four-wire low voltage distribution feeder following a line-to-ground short-circuit fault on the low voltage feeder. Several parameters are considered including the location of the fault, the impedance of the fault and the ratio of the PVs generation capacity to the load demand. Moreover, the impact of the system earthing was analyzed for the multiple earthed neutral and non-effectively grounded systems.

The analyses demonstrate that following a line-to-ground short-circuit fault on one of the phases, the voltages of all nodes along the faulty phase drop below 88% of the nominal voltage immediately. Hence, all the PVs connected to the faulty phase sense the fault and disconnect. The analysis show that the level of voltage drop in the MEN systems is much larger than the NEG system; however, in both cases, the PVs of the faulty phase disconnect in less than a cycle after the fault, if the fault impedance is small (i.e. less than 2 Ω). It was also revealed that the location of the fault, when varied from the beginning of the feeder towards its end as well as the ratio of the generation capacity of PVs versus the load demand, when varied from 50% to 200%, does not have a significant effect on the disconnection of the PVs. It was noticed that there is a possibility for the PVs connected to the faulty phase not to disconnect if the system is NEG and the fault impedance is high (e.g. 20 Ω).

The analyses also demonstrate that the voltages of all nodes along the healthy phases rise above the nominal voltage immediately. The level of voltage rise is higher for the MEN systems compared to the NEG system. Once the voltage magnitude rises above 110% of the nominal voltage, the PVs connected to the healthy phases disconnect. The analyses show that this usually happens in less than a cycle after the fault occurrence. For the healthy phases, it was noticed that the fault impedance has a significant effect on the PVs disconnection. As an example, the analysis revealed that for fault impedance of larger than 2 Ω for the MEN system and larger than 0.2 Ω for the NEG system, the voltage profile along the healthy phases does not rise above 110%. The analyses show that the location of the fault and the ratio of PVs generation to load demand do not have a strong effect on the PVs disconnection.

APPENDIX

The parameters of the network under consideration in Fig. 1 are given in Table A1.

Table A1. Technical data of the network under consideration.

Distribution Transformer	150 kVA, 50 Hz, Dyn-type, Z = 5%
MV feeder	11 kV, 2 km, ACSR 50 mm^2 bare conductor, three-phase three-wire system R = 2.16 Ω/km, X = 2.85 Ω/km [25]
LV feeder	415 V, 400 m, AAC 75 mm^2 bare conductor, three-phase four-wire system with ABCN horizontal configuration on 120 cm crossarms, R = 0.452 Ω/km, X = 0.27 Ω/km [25]
PV inverters	PF = 1, η =100%, $I_{\text{max at Fault}}$ = 150% I_{rated}
Residential House Demand	S = 4.4 kVA, PF = 0.95 lagging Constant Impedance type

REFERENCES

[1] The critical decade: Australia's future –solar energy, 2013. http://www.climatecouncil.org.au/uploads/497bcd1f058be45028e3df9d020ed561.pdf

[2] F. Shahnia, R. Majumder, A. Ghosh, *et al.*, "Voltage imbalance analysis in residential low voltage distribution networks with rooftop PVs," *Electric Power Systems Research*, Vol. 81, Issue 9, pp. 1805–1814, 2011.

[3] K. Kauheniemi and L. Kumpulainen, "Impact of distributed generation on the protection of distribution networks", 8th IEE Int. Conf. on Developments in Power System Protection, Vol. 1, pp. 315–318, April 2004.

[4] M. Patsalides, G.E. Georghiou, A. Stavrou, V. Efthimiou, "Assessing the power quality behavior of high photovoltaic (PV) penetration levels inside the distribution network", 3rd IEEE International Symposium on Power Electronics for Distributed Generation Systems," (PEDG), pp. 709–716, 2012.

[5] W. Peng, S. Haddad, Y. Baghzouz, "Improving power quality in distribution feeders with high PV penetration through inverter controls," Integration of Renewables into the Distribution Grid, CIRED Workshop. 2012.

[6] M.A. Eltawil and Z. Zhao, "Grid-connected photovoltaic power systems: Technical and potential problems-A review," *Renewable & Sustainable Energy Reviews*, Vol. 14, pp.112–129, 2010.

[7] N. Jabalameli, M. Masoum, T. Mehr, F. Shahnia, "Impact of battery rating on performance of rooftop PV supporting household loads, regulating PCC voltage and providing constant output power to grid," 23rd Australasian Universities Power Engineering Conference (AUPEC), pp.1-6, 2013.

[8] N. Jabalameli, N. Deilami, S. Masoum, F. Shahnia ,"Rooftop PV with battery storage for constant output power production considering load characteristics," 8th International Conference on Electrical and Electronics Engineering. (ELECO), Turkey, Nov. 2013.

[9] M.E. Baran, H. Hooshyar, H. Shen, *et al.*, "Impact of high penetration residential PV systems on distribution systems", IEEE Power and Energy Society General Meeting, July 2011.

[10] H. Hooshyar, M. Baran, L. Vanfretti, "Coordination assessment of overcurrent relays in distribution feeders with high penetration of PV systems," IEEE PowerTech. Conference, pp.1–6, 2013, France.

[11] V. Calderaro, S. Corsi, V. Galdi and A. Piccolo, "Optimal setting of the protection systems in distribution networks in presence of distributed generation," 40th Int. Universities Power Engineering Conf. (UPEC), Sept. 2005.

[12] H.H. Yengejeh, F. Shahnia and S. Islam, "Contributions of single-phase rooftop PVs on short circuits faults in residential feeders," 24th Australasian Universities Power Engineering Conference (AUPEC), Australia, Oct 2014.

[13] M.E. Baran, H. Hooshyar, H. Shen, *et al.*" Impact of high penetration residential PV systems on distribution systems," IEEE Power and Energy Society General Meeting, July 2011.

[14] H. Hooshyar and M.E. Baran, "Fault Analysis on Distribution Feeders With High Penetration of PV Systems" *IEEE Transactions on Power Systems*", Vol. 28, Issue 3, pp. 2890-2896, 2013.

[15] T.G. Alvin, I.Z. Abidin, H. Hashim and A. Zainul Abidin, "Phase comparison protection for distribution networks with high PV penetration," Innovative Smart Grid Technologies-Asia, pp. 216–221, 2014.

[16] Ben Noone, "PV integration on Australian distribution networks: Literature review," The Australian PV Association, 2013.

[17] Earthing of the distribution network, Technical Standard TS 109, SA Power Networks, March 2014.

[18] D. Dong, Z. Qi and Y.H. Yang, "Non-effectively grounded system line selection device based on ARM," China Int. Conf. on Electricity Distribution (CICED), pp. 1-6, Dec. 2008.

[19] Western Australian Distribution Connections Manual, 2015. http://www.westernpower.com.au/documents/WA_Distribution_Connections_Manual.pdf

[20] T.A. Short, *Electric power distribution handbook*, CRC Press, 2004.

[21] Distribution construction standards handbook, Part 6: Low voltage overhead, WesternPower, 2007. http://www.westernpower.com.au/documents/low-voltage-overhead-distribution-construction-standards-han.PDF

[22] IEEE Recommended Practice for Utility Interface of Photovoltaic (PV) Systems, IEEE Std 929-2000.

[23] http://www.solarchoice.net.au/blog/residential-solar-pv-system-prices-may-2015

[24] http://www.westernpower.com.au/land-developers-designers-residential-dadmd-calculator.html

[25] Olex aerial conductors catalogue, 2012. http://www.olex.com.au/Australasia/2012/OLC12641_AerialCat.pdf